

01 Jan 2005

## EMI Specifics of Synchronous DC-DC Buck Converters

Zhe Li

David Pommerenke

Missouri University of Science and Technology, davidjp@mst.edu

Follow this and additional works at: [https://scholarsmine.mst.edu/ele\\_comeng\\_facwork](https://scholarsmine.mst.edu/ele_comeng_facwork)



Part of the [Electrical and Computer Engineering Commons](#)

---

### Recommended Citation

Z. Li and D. Pommerenke, "EMI Specifics of Synchronous DC-DC Buck Converters," *Proceedings of the 2005 International Symposium on Electromagnetic Compatibility, 2005. EMC 2005*, Institute of Electrical and Electronics Engineers (IEEE), Jan 2005.

The definitive version is available at <https://doi.org/10.1109/ISEMC.2005.1513616>

This Article - Conference proceedings is brought to you for free and open access by Scholars' Mine. It has been accepted for inclusion in Electrical and Computer Engineering Faculty Research & Creative Works by an authorized administrator of Scholars' Mine. This work is protected by U. S. Copyright Law. Unauthorized use including reproduction for redistribution requires the permission of the copyright holder. For more information, please contact [scholarsmine@mst.edu](mailto:scholarsmine@mst.edu).

# EMI Specifics of Synchronous DC-DC Buck Converters

Zhe Li, David Pommerenke  
Electromagnetic Compatibility Laboratory  
Department of Electrical and Computer Engineering  
University of Missouri-Rolla, Rolla, MO 65409

**Abstract**—DC-DC buck converter topology is widely used in computers and telecom applications because of its high power efficiency and multiple DC levels. However, EMI can be an issue because of its fast switching characteristics and large currents. This paper addresses the analysis of radiated EMI problems associated with DC-DC buck converters and evaluates the effectiveness of solutions that minimize the reverse recovery of the Drain-Bulk diode of the synchronous switching MOSFET.

**Keywords**—Synchronous DC-DC buck converters; EMI; reverse recovery

## I. INTRODUCTION

New generations of microprocessors are powered by local low voltages but high currents power supplies. Due to connector and power loss issues power cannot be delivered by a remote power supply at the desired DC voltage. In addition, fast transient current demand requires the power source being located close to the microprocessors.

The most commonly used voltage regulator design is based on the synchronous buck topology. The input power supply voltage is stepped down to the operating voltage needed by the microprocessor. DC-DC converters operate at switching frequencies up to a few MHz. However, due to fast switching and ringing frequency content at FCC failing levels up to 1 GHz has been observed. With regard to the electromagnetic interference, this type of power supply can be a serious concern [1].

The potential EMI problem has been well covered in the literatures [2-4]. By operating a DC-DC converter with a soft switching scheme without disturbing its averaged duty cycle, it is possible to eliminate predominant harmonics present in the input current to reduce overall peak amplitude of the frequency spectrum. The spreading spectrum concept has been applied successfully for the mitigation of conducted harmonic interference of the DC-DC buck converters [2]. Only in the last few years have the researchers turned their interests on the electromagnetic radiation from such devices. Using of high switching frequencies in DC-DC converters allows magnetic components to be minimized but also enhanced the spectrum of EMI caused by interaction of the active components.

This research analyses the emissions and explains design changes that reduces the emissions. Section II shows the test results of the radiated emission measured on a computer system consisting of DC-DC buck converters as its power supplies. In Section III, we present the Joint Time-Frequency Algorithms

used for DC-DC buck converter analysis. Section IV discusses about the solutions adopted to minimize the reverse recovery of the Drain-Bulk diode of the synchronous MOSFET and the associated emission reduction at high frequencies.

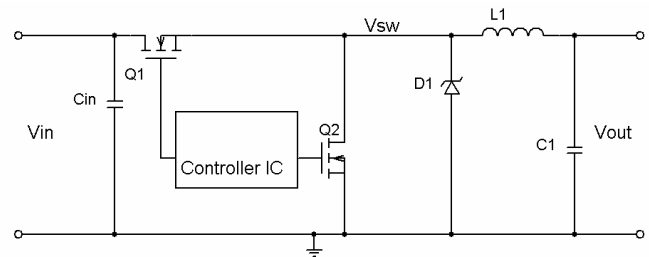


Figure 1. Typical synchronous DC-DC buck converter

## II. RADIATED EMISSIONS

Figure 1 shows the circuit diagram of a typical synchronous DC-DC buck converter. The circuit includes the main control MOSFET switch Q1 and the synchronous MOSFET switch Q2, free wheeling Schottky diode D1, step down inductor L1 and filtering capacitor C1. The two MOSFETs switch on and off in a synchronized pattern:

- After the main control MOSFET switches on, current builds up in the inductor
- After the main control MOSFET switches off, the inductor current freewheels through Schottky diode
- As the synchronous MOSFET turns on, the inductor current is taken over from the diode as the MOSFET offers a lower impedance path. This reduces the losses that occur in the Schottky diode.

The reference measurements and the simulations are based on a multi-chip power module that includes the two MOSFET transistors, Schottky diodes, on-chip decoupling capacitors and the high-speed gate drive controller IC. The PWM controls 4-phase interleaved synchronous buck converters that operate up to 1 MHz per phase. The average power that the synchronous buck regulators provide to the microprocessor is over 120 W.

The measurements on radiated emissions of the synchronous buck converters were designed to investigate the wideband and transient events using conventional temporal and spectral analysis, and Joint Time Frequency Analysis (JTFA) techniques. Our intension of applying the JTFA method is to

extract time-varying information on the emissions from different switching activities of DC-DC buck converters.

First, measured and simulated switching outputs of the power IC are shown in Figure 2. The voltage oscillation on  $V_{sw}$  at the switching output node results from the high  $dv/dt$  at the rising edge of the control MOSFET. The ringing is determined by the combination of the switch node capacitance and the total inductance of the current path [5]. Its resonance frequency is at about 185 MHz.

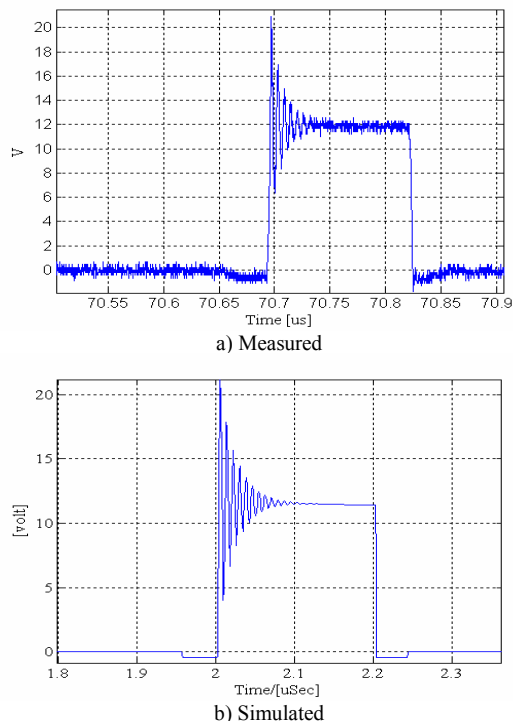


Figure 2. Measured and simulated switching output voltage from the power IC module

Far-field emission measurements are made to determine the relative noise level from the computer system. Signal are captured by a log-periodic antenna in a 3-meters semi-anechoic chamber. As shown in Fig. 3, there are a few broadband frequency components at about 100 MHz, 185 MHz, 260 MHz, 500MHz and 850 MHz. It is not distinguishable for conventional temporal and spectral analyses to tell which frequency component is from which DC-DC buck converters, when exactly in the switching cycle it occurs or if it is from other broadband sources.

The 850 MHz emissions are of special importance, although their level is less than the level of the emissions at lower frequencies. The data in Fig. 3 has been taken without enclosure. The enclosure would shield the lower frequencies significantly better than the 850 MHz, thus the 850 MHz will be the dominating emission in the fully assembled system.

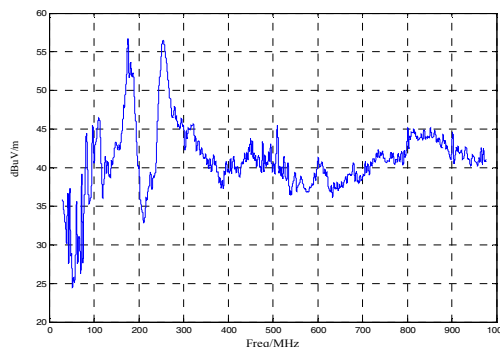


Figure 3. Far-field spectrum of the system from 30 MHz to 1 GHz

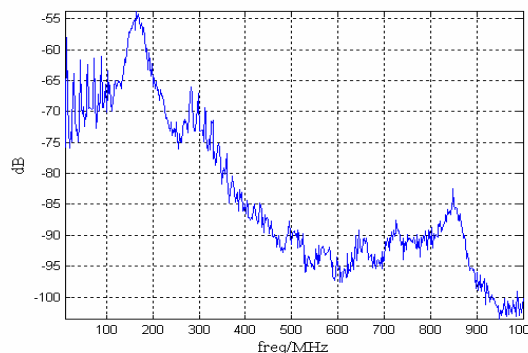


Figure 4. Near-field spectrum of the power IC

A near-field measurement on the Power IC is used to identify noise currents within the power IC. Fig. 4 shows the results of the near-field spectrum captured with a small magnetic loop. The small loop scans on top of the IC and feeds the signal into the spectrum analyzer. The broadband components at 185 MHz and 850 MHz can be identified in both the near and the far field measurement. The location of strongest near field corresponds to the location of the associated switching semiconductor within the IC.

### III. JTFA

In the first section, we present the Joint Time-Frequency Algorithms used in our paper. The principle objective of the JTFA is to describe how the frequency components evolve over time. Several algorithms exist to compute the JTFA, such as Wigner-Vill distribution, Gabor expansion, Wavelets and Short-Term Fast Fourier Transformation and etc. These algorithms have suffered a significant increase in the amount of data to compute and store in the real-time analysis. The easiest and the one we will use in this work is STFFT [6].

STFFT works same as conventional Fourier transformation with short block length, sliding along with full or partial overlap. By taking the Fourier Transformation of the windowed data as the window is moved in time, a two-dimensional time-frequency image, or time-dependent spectrogram, is generated. This spectrogram provides information on the frequency components of the signals evolving with time.

A long record of time domain data was taken and processed by STFFT implemented using Matlab. All data presented are based on data lengths of 6.4M points at 20Gs/s sampling rates, applying a Hamming sliding window of 512 points and using 128 points overlap between adjacent data segments. The result is shown in Fig. 5. JTFA results show that the emission level from the system bursts at a particular time instance which is correlated then to every switching-on event of the buck converter. The 185 MHz and 850 MHz occur at the same time when control MOSFET starts to switch on. This correlation between converter switching event and its emission spectrum is clearly revealed when using the JTFA.

In order to understand the advantages presented by this method against conventional spectral analysis, the STFFT analysis of the switching output waveform is shown in Figure 6. The switch-on event of the control MOSFET occurs every 1 us and excites ringing in the power IC at frequencies of 185 MHz and 850 MHz. The 185MHz component is caused by the MOSFET drain-source capacitance and parasitic loop inductances. Careful observation of the emission profile and switching output waveform of the buck converters shows that the 850 MHz causing event is a result of the reverse recovery of the body diode associated with the synchronous MOSFET [7].

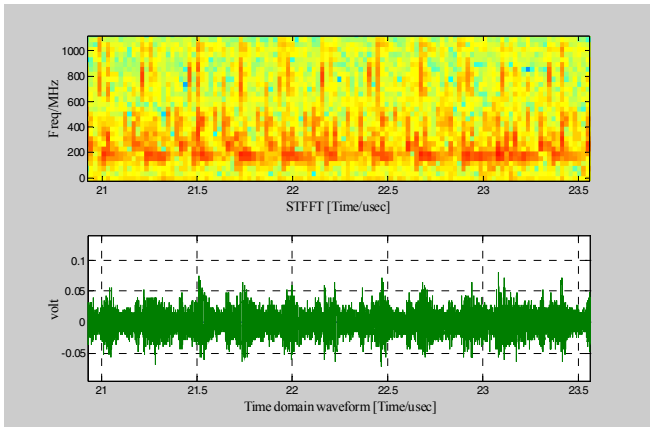


Figure 5. STFFT of the far-field time domain data

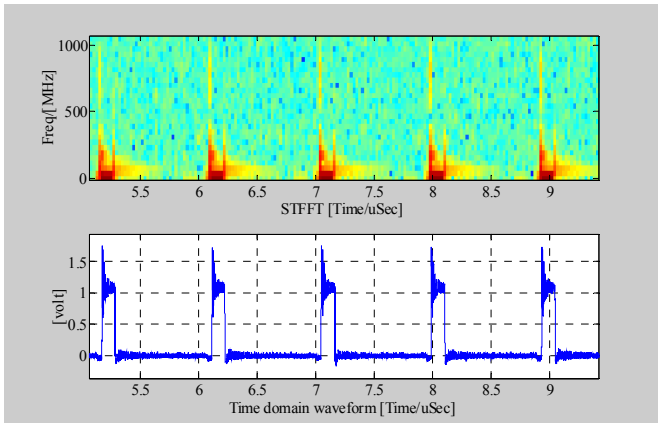


Figure 6. STFFT of the switching output

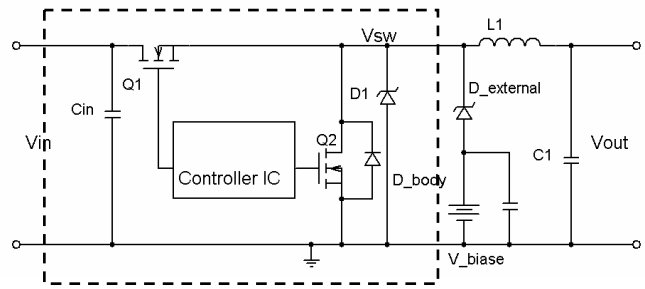


Figure 7. Schematic of the power IC with external Schottky diodes

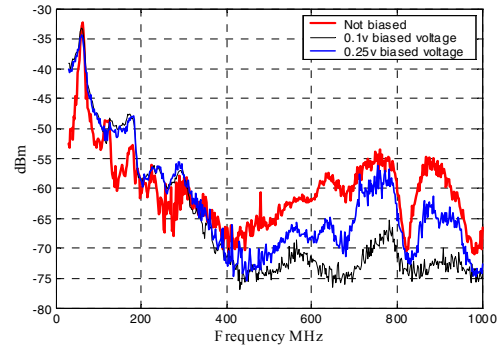


Figure 8. Far field emissions under different bias voltages

#### IV. REVERSE RECOVERY

Most manufacturers reduce the size of the on-chip Schottky diodes to maximize the MOSFET active area. However, the reduced size Schottky diodes may not be capable to carry a fully rated inductor current. At current levels above the Schottky diode rating, the current in the synchronous buck regulator starts to conduct through the MOSFET body diode and leads to a stronger reverse recovery [8].

The reverse recovery of the body diode will cause the high frequency noise by rapidly injecting minority carriers into an LC structure formed by parasitic elements. An experimental setup proves that the MOSFET body diode is causing the 850 MHz emissions. In this experiment, a secondary path is created such that the inductor current is diverted from the IC. Due to a DC-biasing method, it is possible to adjust the current sharing between the external path and the path internally to the IC.

The circuit diagram is shown in Figure 7. A DC biased voltage is applied to enforce the current to go through the external Schottky diode D1. The emission spectrum of the DC-DC converter circuits is shown in Figure 8. The higher the DC biased voltage, the lower the emission at 850MHz.

Reverse recover current has multiple negative effects: It is a source of radiated emission; further, it reduces the efficiency of the DC-DC buck converter. Designers have been trying to implement new techniques to mitigate the effects of the reverse recovery. One of the new power ICs, as shown in Fig. 9, includes monolithically integrated Schottky diodes in the MOSFET cell arrays. The trench area is controlled to increase the reverse current capability of the Schottky diode.

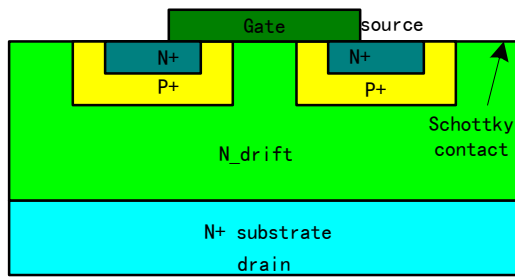


Figure 9. New MOSFET with integrated Schottky contact

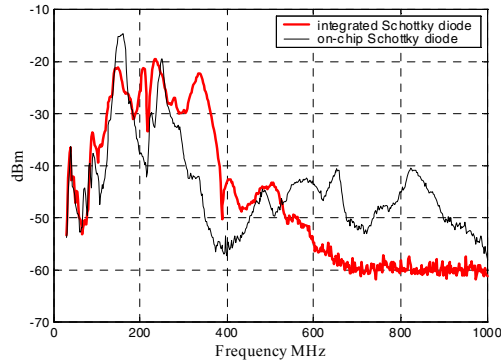


Figure 10. Far-field emissions with integrated Schottky contact

The radiated emission spectrum of a similar converter with the new power IC is shown in Figure 10. The 850 MHz emissions are drastically reduced. Figure 11 displays the STFFT of the switching output waveform. The 850 MHz event used to be present after the rising edge of the control MOSFET turn-on is obviously removed.

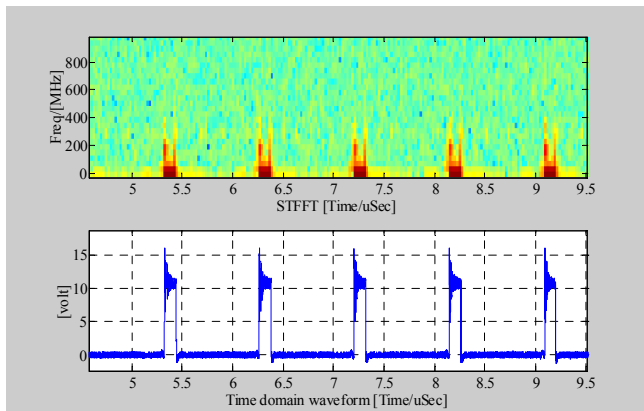


Figure 11. Switching output with integrated Schottky contact

## V. CONCLUSION

The measurement results are typical of those seen for this particular type of synchronous buck converters. To adequately characterize the interference potential of a synchronous DC-DC buck converter it is therefore necessary to correlate the time-

domain behavior and emission spectrum components. JTFA enables significant extra information to be gained over the conventional method.

The effect of body diode conduction and reverse recovery on synchronous MOSFET has been discussed. Reverse recovery not only reduces the power efficiency of the buck converter, but also releases the energy in the form of the electromagnetic field and increase the noise level of the synchronous DC-DC buck converters. A new technique with monolithically integrated Schottky diodes is introduced for reducing the reverse recovery and its related EMI radiation.

## ACKNOWLEDGEMENT

The authors would like to thank David Jauregui at IRF (International Rectifier) for providing valuable help and support in understanding the techniques with their power MOSFETs.

## REFERENCE

- [1] F.L. Luo, Hong Ye, "Investigation of EMI, EMS and EMC in power DC/DC Converters," Power Electronics and Drive Systems, 2003. Volume: 1
- [2] M. Vilathgamuwa, J. Deng, K.J. Tseng, "EMI suppression with switching frequency modulated DC-DC converters," Industry Applications Magazine, IEEE, Volume: 5, Issue: 6, Nov.-Dec. 1999 Pages:27 - 33
- [3] M.H. Nagrial, A. Hellany, "EMI/EMC issues in switch mode power supplies (SMPS)," Electromagnetic Compatibility, 1999 Pages:180 - 185
- [4] C. Kraft, "Conducted noise from 48 volt DC-DC converters used in telecommunications systems and its mitigation for EMC" Telecommunications Energy Special, 2000 Pages:327 - 331
- [5] Mark Pavier, Andrew Sawle, "High frequency DC/DC power conversion: The influence of package parasitics," APEC 2003
- [6] S. Qian, D. Chen, "Joint time-frequency analysis," Signal Processing Magazine, IEEE, Volume: 16, Issue: 2, March 1999
- [7] T. Tolle, T. Duerbaum, R. Elferich, "Switching loss Contributions of synchronous rectifiers in VRM applications," Power Electronics Specialist, 2003 Pages:144 - 149 vol.1
- [8] Y.C. Liang, R. Oruganti, T.B. Oh, "Design considerations of power MOSFET for high frequency synchronous rectification," IEEE Trans. Power Electronics, Vol 10, No. 3, 1995, Pages:388 - 395